

Functional Connectivity Alterations of the Temporal Lobe and Hippocampus in Semantic Dementia and Alzheimer's Disease

Simon Schwab^{a,d}, Soroosh Afyouni^a, Yan Chen^b, Zaizhu Han^c, Qihao Guo^c, Thomas Dierks^d,
Lars-Olof Wahlund^c and Matthias Grieder^{d,*}

^a*Big Data Institute, Li Ka Shing Centre for Health Information and Discovery, Nuffield Department of Population Health, University of Oxford, Oxford, United Kingdom*

^b*State Key Laboratory of Cognitive Neuroscience and Learning, Beijing Normal University, Beijing, China*

^c*Department of Neurology, Huashan Hospital, Fudan University, Shanghai, China*

^d*Translational Research Center, University Hospital of Psychiatry and Psychotherapy, University of Bern, Bern, Switzerland*

^e*Department NVS, Karolinska Institute, Division of Clinical Geriatrics, Stockholm, Sweden*

Handling Associate Editor: Claudio Babiloni

Accepted 27 May 2020

Abstract.

Background: Semantic memory impairments in semantic dementia are attributed to atrophy and functional disruption of the anterior temporal lobes. In contrast, the posterior medial temporal neurodegeneration found in Alzheimer's disease is associated with episodic memory disturbance. The two dementia subtypes share hippocampal deterioration, despite a relatively spared episodic memory in semantic dementia.

Objective: To unravel mutual and divergent functional alterations in Alzheimer's disease and semantic dementia, we assessed functional connectivity between temporal lobe regions in Alzheimer's disease ($n = 16$), semantic dementia ($n = 23$), and healthy controls ($n = 17$).

Methods: In an exploratory study, we used a functional parcellation of the temporal cortex to extract time series from 66 regions for correlation analysis.

Results: Apart from differing connections between Alzheimer's disease and semantic dementia that yielded reduced functional connectivity, we identified a common pathway between the right anterior temporal lobe and the right orbitofrontal cortex in both dementia subtypes. This disconnectivity might be related to social knowledge deficits as part of semantic memory decline. However, such interpretations are preferably made in a holistic context of disease-specific semantic impairments and functional connectivity changes.

*Correspondence to: Matthias Grieder, PhD, Translational Research Center, University Hospital of Psychiatry and Psychotherapy, Bolligenstrasse 111, 3000 Bern 60, Switzerland. Tel.: +41 319328351; Fax: +41 319309961; E-mail: matthias.grieder@upd.unibe.ch.

Conclusion: Despite a major limitation owed to unbalanced databases between study groups, this study provides a preliminary picture of the brain's functional disconnectivity in Alzheimer's disease and semantic dementia. Future studies are needed to replicate findings of a common pathway with consistent diagnostic criteria and neuropsychological evaluation, balanced designs, and matched data MRI acquisition procedures.

Keywords: Alzheimer's disease, functional connectivity, semantic dementia, temporal lobe

INTRODUCTION

Everybody occasionally experiences difficulties in integrating past events into an accurate context—a condition classified as an episodic memory disturbance. Intact episodic memory [1] requires the processing of information about chronology, place, and the protagonists who were involved in an event. The capability to store and retrieve autobiographical memory is, however, not sufficient for an intact episodic memory. Humans also strongly rely on a fully functioning semantic memory. Concretely, semantic memory reflects our general knowledge about concepts such as objects, people, and words. Thus, only a sound interplay of these two memory systems, episodic and semantic memory, allows a cognitively healthy state of an individual.

Previously two initially contradicting models of the neurophysiological organization of semantic memory have been harmonized as what can be characterized as a 'cortically distributed plus semantic hub' theory [2, 3]. The term "distributed" refers to the idea that regions which process semantic concepts receive multimodal input from corresponding brain regions (e.g., visual attributes from visual brain regions, tactile attributes from the sensorimotor cortex, etc.). Subsequently, these multimodal inputs from distributed cortical areas converge to so-called unitary semantic concepts in the semantic hub [4, 5]. The semantic hub was found to be localized bilaterally in the anterior temporal lobe, a region which is atrophied and hypometabolized in patients with the semantic variant of primary progressive aphasia, also known as the temporal variant of frontotemporal dementia (FTD) or semantic dementia (SD) [5–7]. In SD, the onset of gray matter atrophy occurs in the anterior temporal lobes, frequently with an asymmetry toward the more affected left hemisphere. With progression of the disease, the temporal pole and medial as well as lateral temporal areas are degenerated [8]. However, the patients seem to exhibit an almost intact episodic memory, when tested non-verbally, while their semantic memory is severely deteriorated [9, 10].

In contrast to SD, patients with Alzheimer's disease (AD) show predominantly episodic memory impairments, and semantic memory deficits can only be observed to a minor degree [11–13]. AD has been described as a disconnection syndrome, that is, connections of functionally or structurally linked brain regions that are part of a network become increasingly disrupted [14–16]. This degenerative mechanism has been associated with the cognitive deficits of patients with AD [17–19]. A common finding in AD is that gray matter atrophy onset can be localized in the hippocampal, posterior cingulate, and lateral parietal brain regions, as well as in the amygdala [20, 21]. The hippocampus forms a core region for episodic memory encoding. However, it has also been associated with semantic memory functions [22]. In fact, Burianova and colleagues [22] postulated that the hippocampus is part of a *common* declarative memory network, suggesting that the hippocampus has a key role in both semantic as well as episodic and autobiographical memory.

The properties of functional systems, as for example Burianova and colleagues' proposed declarative memory network, are commonly assessed by the use of a resting-state functional connectivity (FC) analysis. The human resting-state is characterized by spatially discriminate brain regions that co-activate and deactivate at a low temporal frequency, commonly known as resting-state networks [23, 24]. These functional systems, or resting-state networks, are commonly assessed using blood-oxygen level dependent resting-state fMRI. It has become very popular to study FC alterations in various mental and neurological disorders including AD, demonstrating a relationship between disease and abnormalities in resting-state networks [25–27].

FC changes (i.e., decreases and increases of connectivity strengths) in AD have been found predominantly in the hippocampus and the default mode network [28–31]. With the progression of the disease, structural and functional connectivity distortions affect several networks, particularly those involving the para hippocampus [17, 32]. In SD, FC appears to be deteriorated in regions either affected

117 by or proximate to the core of atrophy, located in
118 regions such as the temporal pole, anterior middle
119 temporal gyrus, inferior temporal gyrus, and insula
120 [6, 33–35]. Furthermore, reduced FC of the anterior
121 temporal lobe with various cortical regions was also
122 found in SD [2].

123 Considering these findings as well as the distinct
124 pathology of AD and SD, it is likely that the neuronal
125 loss of hippocampal cells that results in gray matter
126 atrophy certainly affects the functional networks in
127 a way that generates episodic memory deficits. Tem-
128 poral pole atrophy alone might not be necessary (but
129 sufficient) to lead to semantic impairment. Follow-
130 ing these findings, La Joie et al. [36] identified the
131 hippocampus as the ‘main crossroad’ between brain
132 networks that are disrupted in AD and SD. Despite the
133 growing body of research, the common and divergent
134 changes of FC among regions of the temporal lobes
135 in AD and SD are not fully understood. A caveat
136 when interpreting the existing literature is the com-
137 mon use of anatomical/structural parcellation instead
138 of a functional parcellation to study FC. Functional
139 parcellations have the advantage that the resulting
140 functional regions of interest (ROIs) are homoge-
141 neous, i.e., the voxels have similar time courses. On
142 the other hand, parcellations based on brain structure
143 can merge the time series across functionally different
144 areas which can be problematic [37].

145 This proof-of-concept study aimed at disentangling
146 FC alterations of the temporal lobe in AD and
147 SD using a refined division of temporal subregions:
148 sixty-six functional regions of interest (ROIs) of the
149 temporal lobes from a functional atlas [38]. In con-
150 trast to numerous previous studies, we accounted for
151 structural changes (i.e., gray matter density) in order
152 to extract FC time series data from preserved gray
153 matter tissue which can still be functional [39, 40].
154 In other words, results from the FC analysis reflect
155 the functional reorganization of the temporal lobes
156 affected by atrophy.

157 A common issue with studies involving patients
158 with SD is the small sample size due to the low
159 prevalence and relatively difficult diagnosis. In order
160 to overcome this to some extent, we pooled two
161 data sets from two different recording sites (see
162 Method section for details). Orban et al. [41] showed
163 the advantage of multisite fMRI-data in multivariate
164 fMRI analysis. Their approach appears to be gener-
165 alizable; however, in our study, we were not able to
166 accomplish an evenly matched number of patients or
167 controls at each MRI scanner site, which is a prereq-
168 uisite for a correct experimental design. In particular,

169 the circumstance that the majority of SD patients was
170 scanned at the Shanghai site and all AD patients and
171 healthy controls (HC) were scanned at the Stock-
172 holm site, increases the likelihood of false positive
173 contrasts between the groups due to instrumental arti-
174 facts. Other inherent limitations will be addressed in
175 the discussion section (e.g., site-specific diagnostic
176 criteria, neuropsychological testing, and fMRI acqui-
177 sition procedures).

178 Despite the exploratory analysis approach to test
179 all possible connections, based on previous find-
180 ings described above, the following hypotheses were
181 tested: in AD, we expected FC alterations in the
182 hippocampus, parahippocampal ROIs, and possibly
183 posterior temporal ROIs. In SD, altered FC was antic-
184 ipated in the hippocampus, the fusiform gyrus, and
185 the temporal pole.

186 METHODS

187 *Participants*

188 We analyzed resting-state fMRI data from a total of
189 62 participants from three groups: semantic demen-
190 tia (SD), Alzheimer’s disease (AD), and a healthy
191 elderly control group (HC). We examined all the
192 functional MRI data and excluded six datasets due
193 to insufficient data quality (see data quality con-
194 trol). The final sample consisted of 56 participants:
195 Twenty-three patients with SD, with a mean age
196 (\pm standard deviation) of 62 ± 7.6 , 16 patients with
197 AD, mean age of 70 ± 8.5 , and 17 individuals in
198 the HC group, mean age 70 ± 3.4 ; see Table 1 for
199 demographics and clinical variables. Patients with
200 SD from the Stockholm site ($n=7$) were recruited
201 throughout Sweden and diagnosed using the crite-
202 ria of Neary et al. [42], while patients with SD
203 from Shanghai were recruited from Huashan Hos-
204 pital in Shanghai ($n=19$), according to the criteria
205 of Gorno-Tempini et al. [43]. The main diagnostic
206 criteria of both guidelines share clinical observation
207 features such as impaired word naming and com-
208 prehension, spared repetition, and surface dyslexia
209 and dysgraphia. Differences in these two diagnos-
210 tic criteria, as for instance the introduction of brain
211 imaging as a supportive diagnostic feature in Gorno-
212 Tempini et al. (2011), were not relevant, because
213 also the Swedish patients underwent MRI to assess
214 anterior temporal lobe atrophy. Patients with AD
215 were recruited at the Memory Clinic of the Geri-
216 atric Department at Karolinska University Hospital
217 in Huddinge, Sweden ($n=19$). Their diagnosis was

Table 1

Descriptives and clinical scores. Kruskal-Wallis tests were run to assess group differences of age, education, MMSE, BNT, lexical decision, AF, and VF. Comparisons between AD and SD of the CDS and GDS scores were performed using the non-parametric Kolmogorov-Smirnov-Test

| | HC (<i>n</i> = 17) | Normative data [†] | AD (<i>n</i> = 16) | SD (<i>n</i> = 23) | <i>p</i> |
|----------------------------------|--------------------------|-----------------------------|---------------------------|-------------------------------|----------|
| | Mean (std. dev.) | Mean (std. dev.) | Mean (std. dev.) | Mean (std. dev.) | |
| Age, y | 67.9 (3.3) | | 68.4 (8.5) | 61.5 (7.4) | 0.004 |
| Gender (F:M) | 12 : 5 | | 7 : 9 | 10 : 13 | – |
| Education, y | 13.9 (3.1) | | 13.1 (3.0) | 12.4 (1.5) ³ | 0.61 |
| CDS | – | | 1.0 (1.0) | 1.8 (2.2) ³ | 0.60 |
| GDS | – | | 2.9 (0.8) | 3.8 (0.4) ³ | 0.031 |
| MMSE (max 30) | 28.8 (0.8) | | 24.5 (4.8) | 20.8 (5.2)⁴ | <0.0001 |
| BNT (max 60) | 54.4 (3.7) | 54.0 (4.5) | 45.6 (6.5) | 8.2 (5.7) ³ | <0.0001 |
| Oral picture-naming (max 140) | – | | – | 39.2 (27.6) ⁵ | – |
| Word-triple association (max 70) | – | | – | 51.2 (10.1) ⁵ | – |
| Number calculation task (max 7) | – | | – | 6.36 (1.1) ⁵ | – |
| Lexical decision (max 352) | 346.0 (3.7) ¹ | | 333.2 (23.5) ² | 325.3 (23.0) ⁶ | 0.002 |
| AF, animals/min | 23.8 (5.9) | 18.2 (3.8) | 14.1 (4.2) | 5.6 (4.3) ³ | <0.0001 |
| VF, verbs/min | 21.9 (5.8) | 18.2 (5.6) | 11.9 (5.0) | 7.0 (2.8) ³ | <0.0001 |

[†] Normative data are reference values for comparison of the control group (HC) with respect to BNT with *N* = 32 [81]; AF with *N* = 94 [82]; VF with *N* = 67 [83]. ¹*n* = 16, ²*n* = 12, ³*n* = 5, ⁴*n* = 19, ⁵*n* = 14, ⁶*n* = 4. CDS, Cornell Depression Scale; GDS, Global Deterioration Scale; MMSE, Mini-Mental State Examination; BNT, Boston Naming Test; AF, animal fluency; VF, verb fluency.

performed by expert clinicians and was in accordance with the ICD-10 criteria [44]. The patients with AD included in this study underwent a standard clinical procedure which consisted of examinations such as structural neuroimaging, lumbar puncture, blood analyses, and a neuropsychological assessment (these assessments were part of the clinical routine and only used for diagnosis). Further inclusion criteria for patients from the Stockholm site was a Global Deterioration Scale lower than 6 (i.e., moderate dementia or milder) and the Cornell Depression Scale below 8. Healthy elderly controls were recruited by advertisement (*n* = 22) in the Stockholm area. Presence of medical or psychiatric disorders (other than dementia), intake of drugs affecting the nervous system, or magnetic implants, led to an exclusion from the study. Variables available for all participants included in the study were age, gender, and Mini-Mental State Examination (MMSE).

All study participants provided informed consent prior to the data acquisition. The Shanghai study was approved by the Institutional Review Board of the State Key Laboratory of Cognitive Neuroscience and Learning, Beijing Normal University [33]. The Stockholm study was approved by the Regional Ethics Committee of Stockholm, Sweden.

MRI data

MR images were acquired on two sites: The Karolinska Institute in Stockholm, Sweden, and the Huashan Hospital in Shanghai, China.

Stockholm site

MR images were acquired with a 3T Siemens Magnetom Trio scanner (Siemens AG, Erlangen, Germany). Structural images were 3D T1-weighted magnetization-prepared rapid gradient echo (MPRAGE) images using the following parameters: TR = 1900 ms, TE = 2.57 ms, flip angle = 9°, matrix size = 256 × 256, field of view = 230 × 230 mm², slice number = 176 slices, slice thickness = 1 mm, and voxel size = 0.90 × 0.90 × 1 mm³. The structural images were previously used for voxel-based morphometry and published with a different purpose and sample configuration [45, 46]. Functional images were acquired with a 32-channel head coil, using an interleaved EPI sequence (400 volumes; 26 slices; voxel, 3 × 3 × 4 mm³; gap thickness, 0.2 mm; matrix size, 80 × 80; FOV, 240 × 240 mm²; TR, 1600 ms; TE, 35 ms).

Shanghai site

Images were acquired with a 3T Siemens Magnetom Verio. Structural images were 3D T1-weighted magnetization-prepared rapid gradient echo (MPRAGE) images using the following parameters: TR = 2300 ms, TE = 2.98 ms, flip angle = 9°, matrix size = 240 × 256, field of view = 240 × 256 mm², slice number = 192 slices, slice thickness = 1 mm, and voxel size = 1 × 1 × 1 mm³. Functional images were acquired with a 32-channel head coil, using an interleaved EPI sequence (200 volumes; 33 slices; voxel, 4 × 4 × 4 mm³; gap thickness, 0 mm; matrix size, 64 × 64; FOV, 256 × 256 mm²; TR, 2000 ms;

TE, 35 ms, flip angle 90°). The data were previously published with a different sample configuration (SD only sample) in a combined structural and functional study using a hippocampus seed region [47], as well as in a structural voxel-based morphometry (VBM) study [33].

Preprocessing of functional MRI scans

We performed pre-processing using SPM12 (<http://www.fil.ion.ucl.ac.uk/spm>). We initially set all images' origin to the anterior commissure, and then performed slice-time correction, realignment, coregistration, normalization to MNI space ($2 \times 2 \times 2 \text{ mm}^3$), and smoothing (full width half maximum [FWHM]; 8 mm). Time series data were high-pass filtered (1/128 Hz) and we regressed out 14 nuisance parameters (6 movement parameters and their first derivative, white matter, and cerebrospinal fluid).

We carefully assessed data quality and inspected the spatio-temporal quality of each scan by comparing the slow and fast components of the data using DSE (Dvar, Svar&Evar) decomposition [48]. The DSE technique decomposes the dataset into three main components: fast, which is the squared mean difference; slow, which is the squared mean averages, and Evar, which refers to the sum of squares of the two ends of the time series. Subjects with remarkably high divergence (>75%-tile) between Dvar and Svar components were removed, as suggested in Afyouni & Nichols [48]. Therefore, we removed one SD and three HC datasets from the analysis. We further excluded two AD subjects, as more than 20% of their DVARS data-point were found to be corrupted. The remaining subjects were scrubbed as suggested by Power et al. [49]. Altogether, we excluded six datasets (9.7%) due to poor data quality. We re-run the diagnostics on the final sample and found no difference between groups regarding the DSE diagnostics (one-way ANOVA, all $p > 0.05$).

Functional connectivity analysis

We investigated FC between each of the 66 temporal ROIs in three participant groups (AD, SD, and HC). We focused our analysis on the temporal lobes with the following rationale: first, brain regions identified as the origin of atrophy are located in the temporal lobe. Second, a 'crossroad' in FC network disruption in AD and SD was found in the hippocampus. Third, functional hubs for episodic and semantic

memory can be found in the temporal lobe (as outlined above). Fourth, the strongest FC of temporal regions is located within the temporal lobes and concurs with functional networks crucial for language processing, the core clinical feature of SD [50]. The functional parcellation we used is based on resting-state fMRI data which was clustered into spatially coherent regions of homogeneous FC and was evaluated in terms of the generalizability of group level results to the individual [38]. From the 200 ROIs, we used a subset of 66 temporal ROIs that covered at least 5% or more of one of the following temporal structures from WFU Pickatlas 3.0.4 [51]: the superior temporal cortex, the middle temporal cortex, the inferior temporal cortex, the temporal pole, the hippocampus, the parahippocampal cortex, the lingual gyrus, the amygdala, the insular cortex, and the fusiform gyrus; these 66 ROIs are shown in Supplementary Figure 1. Analyzing merely 66 temporal ROIs leads to 2,145 pair wise correlations, which necessitates a strong adjustment for multiple comparisons to control for false positives. Using an even higher number of ROIs, for example comparing 200 ROIs in the whole brain, would require an even stronger correction (correcting for almost 20,000 comparisons). Such corrections would result in a sensitivity too low to detect even substantial FC changes.

We extracted the mean time series from the gray matter (probability > 0.70) of these ROIs to assure that time series were not contaminated with cerebrospinal fluid signals from atrophied areas, resulting in 66 time series per subject. We also assured that time series were not affected by signal dropouts due to dephasing. To address motion and physiological confounds which are global in nature, we applied global signal regression to the time series [52–54]. We created a pair-wise correlation matrix and transformed the correlation coefficient to Z-scores by Fisher's transformation. We conducted a one-way ANOVA for each ROI pair (2,145 tests) to test the null hypothesis of no difference between the three groups. We performed an additional sensitivity analysis with age, mean gray matter density in the temporal cortex, MMSE, and study site as additional covariates. Covariates can be problematic if these differ between groups [55], therefore we report these sensitivity analyses in the Supplementary Material. From the 2,145 total connections, we found 321 (sensitivity analysis: 324) significant edges that showed a group effect (uncorrected, $p < 0.05$), and after correcting the p -values for multiple comparisons, seven edges

showed a significant group effect (FDR corrected, $p < 0.05$).

Voxel-based morphometry analysis

We additionally performed a VBM analysis to quantify gray matter loss in the patients from the anatomical T1 images. VBM is a voxel-wise comparison of the local amount of gray matter volume between two groups [56]. We performed the following processing steps: spatial registration to MNI space (voxel size: $1.5 \times 1.5 \times 1.5 \text{ mm}^3$) and tissue segmentation, bias correction of the intensities, smoothing of the GM images with 8 mm FWHM, and modulation by scaling with the total volume so that the resulting amount of gray matter in the modulated images remained the same as in the native images. In other words, this step removed the introduced bias from the registration of different brain sizes to MNI space. The Stockholm sample was registered using the European brain template, the Shanghai sample with the East Asian brain template and normalized to MNI space. We used the “Computational Anatomy Toolbox” CAT12 [57] and SPM12 [58] for the VBM analysis. Statistical inference was performed with the “Statistical Non Parametric Mapping” software SnPM13 using non-parametric permutation/randomization two-sample t -tests with a voxel-wise family-wise error correction (FWE) of 0.05. We performed two t -tests and compared the HC group versus the SD group, and the HC group versus the AD group. Unlike in the analyses of the functional data where we excluded six datasets, the structural T1 scan from all the subjects were used in this analysis, the group sizes were HC with $n = 20$, AD with $n = 18$, SD with $n = 24$.

RESULTS

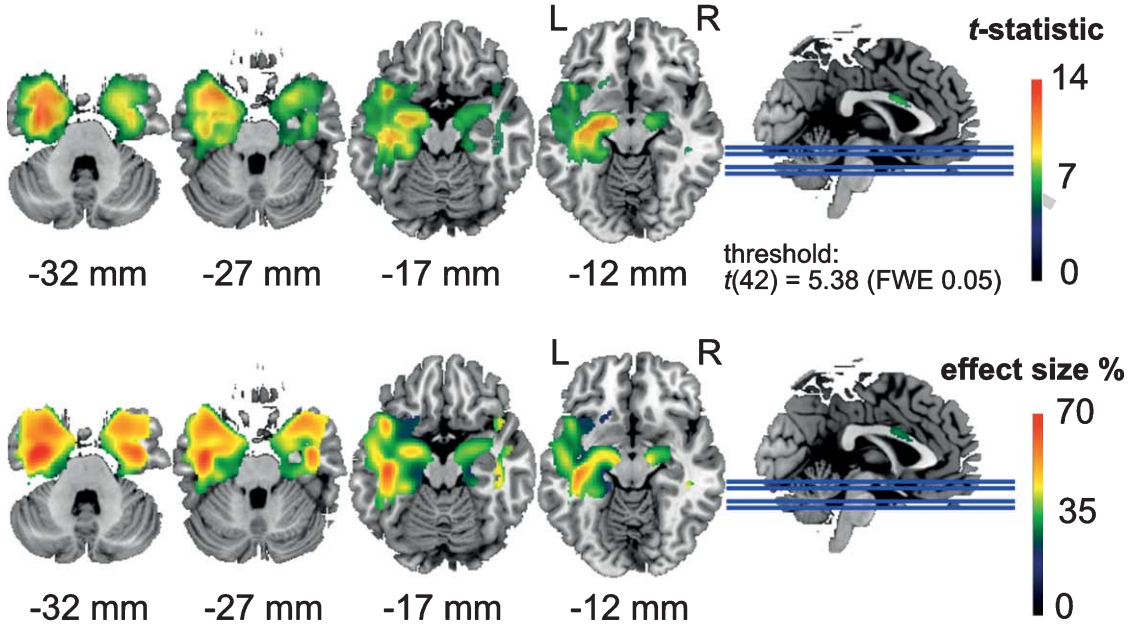
We first describe the clinical presentation of the patients included in this study (see Table 1 for details). The SD group performed poorer in MMSE than the AD group (Kruskal-Wallis over all groups: $H = 29.5$, $df = 2$, $p < 0.0001$; Kolmogorov-Smirnov group-wise *post-hoc* tests: HC-AD $Z = 1.86$, $p = 0.002$, HC-SD $Z = 2.52$, $p < 0.001$, AD-SD $Z = 1.44$, $p = 0.033$). Furthermore, the SD group showed significantly lower scores in the Boston Naming Test (BNT) than the AD group (Kruskal-Wallis over all groups: $H = 23.3$, $df = 2$, $p < 0.0001$; Kolmogorov-Smirnov group-wise *post-hoc* tests: HC-AD $Z = 1.85$, $p = 0.002$, HC-SD $Z = 1.97$, $p = 0.001$, AD-SD $Z = 1.95$, $p = 0.001$).

Within the SD group, we observed that the impaired performance in picture naming (BNT, Stockholm site; oral picture-naming, Shanghai site) were more pronounced than lexical decision (Stockholm site) and word-triple association (Shanghai site), see Table 1. The group differences between SD and AD in MMSE and BNT are common findings given that the BNT is a semantic task and the MMSE relies on language comprehension, as both semantics and language are typically more affected in SD than AD. Finally, our AD group also showed semantic deficits as compared to the healthy control group (based on BNT, animal fluency, and verbal fluency). These behavioral scores mirror the severe semantic memory deficits in patients with SD. Moreover, the normal calculation ability in the majority of our SD group supported the diagnostic features of SD. In contrast, patients with AD showed a comparably mild semantic memory deficit, which is in accordance with the expectations. MMSE was the only available neuropsychological test score for all participants from both sites, whereas the remaining tests were site-specific and therefore not comparable.

Next, we report the gray matter density found in the patient groups, see Fig. 1. In the SD patients (Fig. 1A), we found two clusters of atrophy. The first was located in the left anterior medial temporal cortex, with a peak effect in the left temporal fusiform cortex (peak t -score = 14.0, $p_{\text{FDR}} = 0.0021$, $df = 42$; location at $x = -34$, $y = -3$, $z = -36$; cluster area 80.7 cm^3). The second cluster was located in the temporal fusiform cortex of the right hemisphere (peak t -score = 10.6, $p_{\text{FDR}} = 0.0021$, $df = 42$; location at $x = 34$, $y = -3$, $z = -34$; cluster area 40.1 cm^3). In the AD patients, we found two clusters with lower GM volume compared to controls in the left amygdala (peak t -score = 8.72, $p_{\text{FDR}} = 0.006$, $df = 36$; location at $x = -26$, $y = -10$, $z = -12$; cluster area 7.23 cm^3) and the right amygdala (peak t -score = 7.49, $p_{\text{FDR}} = 0.006$, $df = 36$; location at $x = 22$, $y = -3$, $z = -15$; cluster area 7.47 cm^3), see Fig. 1B. A commonly expected hippocampal atrophy was yielded only with a more liberal threshold (Supplementary Figure 2).

To achieve the main goal of this study, we analyzed the functional connectivity of 56 participants using 66 functional ROIs of the temporal cortex and related sub cortical areas (see complete correlational matrix in Supplementary Figure 3). Seven connections (FC between ROI pairs) demonstrated a significant difference between the three groups after correcting for multiple comparisons (FDR corrected, $p < 0.05$). A detailed characterization and test statistics of these

A Semantic dementia GM atrophy



B Alzheimer's disease GM atrophy

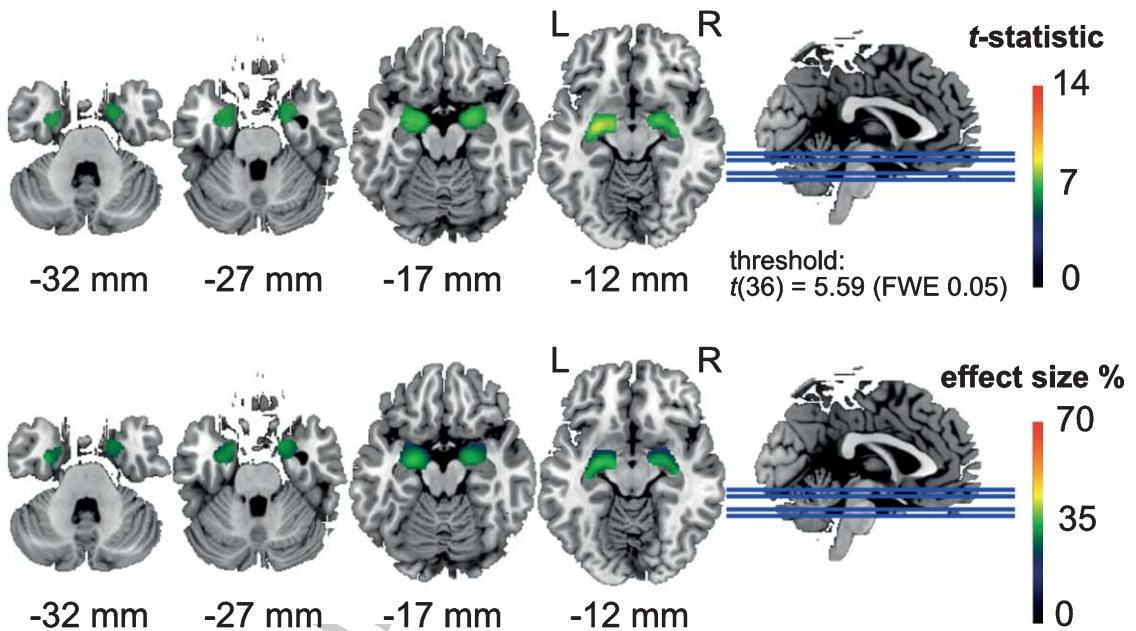


Fig. 1. Areas with significantly lower (voxel-level) gray matter (GM) density (top) and effect size in terms of percentage GM reduction (bottom) in (A) the semantic dementia (SD) patients ($n=24$) and (B) Alzheimer's disease (AD) patients ($n=18$) compared to the healthy elderly control group ($n=20$). SD patients showed reduced GM density in widespread areas of the left anterior temporal cortex including the temporal pole, while the AD patients showed reduced GM density in the amygdala. SD patients showed more severe GM loss with up to 70% reduction, and AD patients with up to 40% reduction in some areas.

Table 2
Seven functional connections that demonstrated significant group differences

| Edge no. | ROI no. | ROI no. | Region | Region | F | FDR adj. p |
|----------|---------|---------|--|--|-------|------------|
| 1 | 129 | 11 | Left anterior superior temporal gyrus/middle temporal gyrus/insular cortex | Left posterior middle temporal gyrus/superior temporal gyrus | 10.86 | 0.034 |
| 2 | 85 | 24 | Right lateral inferior occipital cortex/lateral superior occipital cortex | Left posterior superior temporal gyrus/central opercular cortex/parietal opercular cortex/planum temporale | 11.52 | 0.030 |
| 3 | 198 | 32 | Right fusiform cortex/parahippocampal gyrus | Right inferior temporal pole | 12.64 | 0.026 |
| 4 | 70 | 37 | Left lingual gyrus/intracalcarine cortex/precuneus cortex | Left posterior hippocampus/thalamus | 13.18 | 0.026 |
| 5 | 89 | 37 | Right lingual gyrus/intracalcarine cortex | Left posterior hippocampus/thalamus | 10.95 | 0.034 |
| 6 | 153 | 71 | Right anterior middle temporal gyrus/superior temporal gyrus | Right orbitofrontal cortex | 12.42 | 0.026 |
| 7 | 112 | 72 | Left orbitofrontal cortex/insular cortex | Left anterior inferior temporal gyrus/middle temporal gyrus | 12.06 | 0.026 |

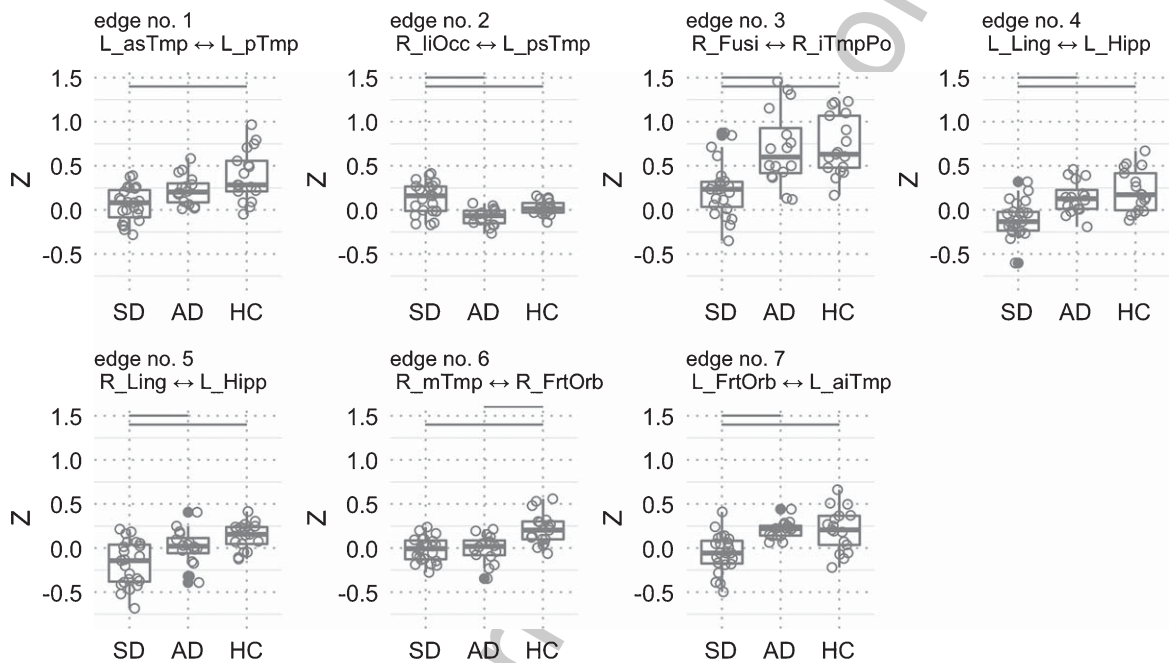


Fig. 2. Z-scores of seven connections (edges 1–7) with significant group differences. *Post-hoc* tests between the three groups were performed, and significant group differences are denoted with red horizontal lines (see Table 2 for a detailed description of the ROIs). Ring-shaped circles represent single subject data points. Filled circles represent outliers.

Table 3

Post-hoc Tukey HSD *p*-values for the three single comparisons (rows) and for each of the seven ROI-pairs that had a significant group effect (columns). Significant values reflect that the group effect was driven by a specific group level contrast

| Edge No. | 1 | 2 | 3 | 4 | 5 | 6 | 7 |
|--------------|---------|---------|--------|---------|---------|---------|--------|
| AD versus HC | 0.098 | 0.082 | 0.98 | 0.54 | 0.22 | 0.0005 | 1.00 |
| SD versus HC | <0.0001 | 0.044 | 0.0002 | <0.0001 | <0.0001 | <0.0001 | 0.0004 |
| SD versus AD | 0.064 | <0.0001 | 0.0004 | 0.002 | 0.024 | 0.97 | 0.0004 |

478 seven connections are shown in Table 2; the Z-values
479 for the significant connections are depicted in Fig. 2.
480 We performed *post-hoc* tests (Tukey HSD) for sin-

gle comparisons of the three groups to investigate the
particular group contrasts that drove the significant
group effect (Table 3). We found that most differ-

481
482
483

ences were related to the SD patients with significant changes in all of the seven connections. SD patients showed lower FC in 6 out of 7 connections compared to HC, and higher FC in one connection (edge no. 2) compared to HC. This higher FC in the SD patients was also significantly higher compared to the AD patients. The AD patients had a lower FC compared to HC patients in only 1 out of the 7 connections (edge 6). Comparing the two patient groups SD, versus AD, we found that SD had a significant lower FC in 4 connections (edges 3, 4, 5, 7).

We visualized the connectivity structure and connection strengths, see Fig. 3. The SD patients generally had a much lower connectivity compared to the other two groups. An exception was the stronger contra lateral connection between the right lateral inferior occipital cortex and the left posterior superior temporal gyrus (edge no. 2). The AD patients showed a lower FC compared to HC between the right middle temporal gyrus and the right frontal orbital cortex (edge no. 6). A common finding in all the three groups was that the FC between the right fusiform cortex and the right inferior temporal pole was the strongest (no. 3).

The sensitivity analysis with age, mean gray matter density in the temporal cortex, MMSE, and study site as covariates produced statistically significant differences in the same seven edges as reported above; however, the assumption of the ANCOVA, the independence between the patient group and the covariates was not met. For results of the sensitivity analysis with covariates, see Supplementary Tables 1–4.

DISCUSSION

In this study, we compared functional connectivity between SD, AD, and HC using a functional parcellation of 66 ROIs of the temporal cortex and hippocampus to investigate intra-temporal connections and connections with contra lateral temporal regions. The overall picture that emerges is that between the majority of the significant ROIs, SD demonstrated the most striking decrease in FC. In the AD group, most differences compared to the HC group did not reach significance. We believe that the often described disconnections found in AD were not detected in our study due to the mild progression of the disease in our AD group. One reason could be that the remaining gray matter volume in brain regions typically affected by neuronal degeneration was suffi-

cient to maintain an intact FC to remote areas. In other words, the damage found in mild stages might affect the intra-regional processing in local neuronal populations, whereas the inter-regional (i.e., network) FC would be affected during more advanced AD progression [59]. Future studies will require larger sample sizes to demonstrate smaller changes in FC seen even with mild state impairments.

The most intriguing finding of our study for the SD group was the decreased FC between the left posterior hippocampus and left/ right lingual gyri (edges 4 and 5). These disruptions are characteristic for the neurophysiological basis of the SD patients' typical symptomatology involving an impaired semantic memory. For instance, Sormaz et al. [60] recently showed a correlation of FC between left the hippocampus and the lingual gyrus with topographic memory, and a correlation of semantic memory performance with FC to the intracalcarine cortex, a finding consistent with our results.

Functional connectivity between the left anterior superior/middle temporal gyrus/insula and the left posterior middle/superior temporal gyrus was decreased in SD compared to HC (edge no. 1). It is important to note that this is the single connection that showed an FC difference between SD and HC exclusively (i.e., a finding specific for the SD-HC group single-comparison while neither AD-HC nor AD-SD were significant). These regions are commonly associated with cross-modal integration (as is the hypothesized semantic hub) of auditory and language processing, as well as the processing of the emotionally relevant context. Hence, this finding might reflect the severe semantic deficits in SD (see Table 1) that are manifested by the loss of conceptual knowledge [7].

The single connection that showed increased FC in SD compared to the other groups (edge no. 2) was between the left posterior superior temporal gyrus/parietal opercular cortex/planum temporale and the right lateral inferior/superior occipital cortex. The temporal brain areas that constitute this connection are important for early context integration of acoustically presented words [61], lexico-semantic retrieval [62], and are part of a supramodal semantic network [63]. The occipital ROI of this connection sub serves visual integration. Thus, an increased FC between these regions might reflect a functional reorganization that is characterized by supporting language comprehension using more sensory inputs. Moreover, this result indicated a reduced hemispheric functional specialization and perhaps an attempt to pool

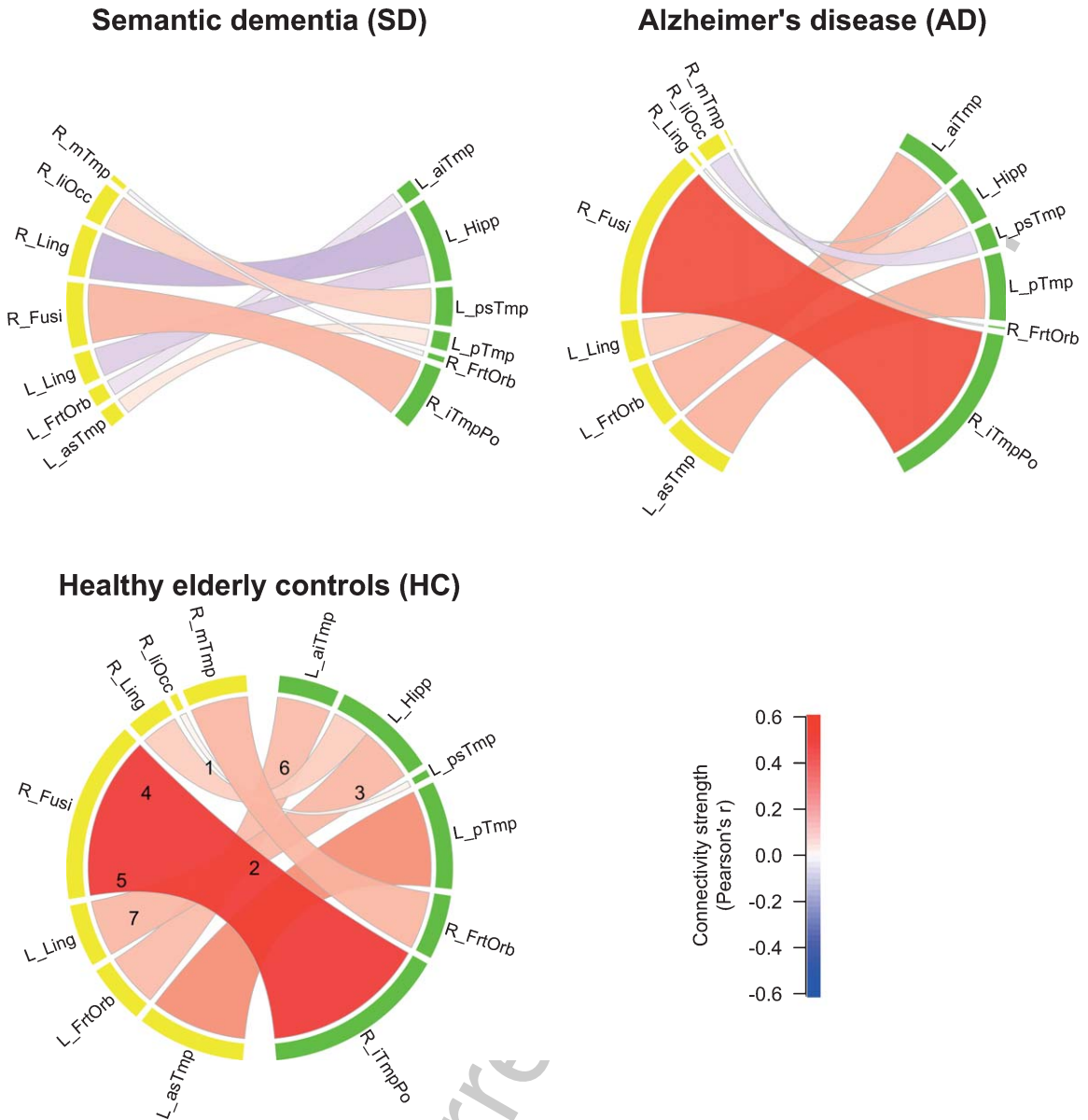


Fig. 3. Functional connectivity (FC) strengths of the three groups. Color shades and thickness of the links are proportional to FC strengths; shades of red reflect positive, shades of blue negative strengths. Numbers in HC group indicate edge numbers (see Table 2 for a detailed description of the ROIs). ROIs in the left hemisphere are labeled yellow, ROIs in the right hemisphere labeled green.

resources that are spared by the pathological developments in SD.

In comparison with AD and HC, SD patients showed a lower FC between the functional ROI encompassing the right fusiform/parahippocampal gyri and the right inferior temporal pole. Disruption of this connection (no. 3) can be viewed as SD-typical, as the functional profile of the involved regions conforms to SD symptomatology. In particular, the right temporal pole is crucial for non-verbal

(e.g., visual) object recognition, which is a hallmark impairment in SD associated with the loss of semantic knowledge [64, 65]. The right fusiform gyrus on the other hand is associated with working memory for faces, face perception, and non-verbal associative semantic knowledge [66–68], and the right parahippocampal gyrus is associated with working memory for object location as well as a function as an episodic buffer [69, 70]. In line with this, the patients with SD in the present study showed severe object recognition

605 deficits assessed with BNT and oral picture-naming
606 (Table 1), even though no behavioral data about face
607 perception or non-verbal semantic knowledge was
608 available.

609 Similar to connection no. 3, FC was reduced
610 in SD compared with AD and HC between the
611 ROI comprising left lingual/intracalcarine/precuneus
612 cortex and the ROI including left posterior hippocam-
613 pus/thalamus (connection no. 4). This finding is in
614 line with Seeley et al. [14], who reported the medial
615 temporal lobe as part of an SD-vulnerable network.
616 Thus, in addition we showed a possible contribu-
617 tion of the primary visual (intracalcarine cortex),
618 visual memory (lingual gyrus) and self-awareness
619 (precuneus, i.e., default mode network) regions to that
620 semantic network. It might appear surprising that the
621 FC of the AD group was not significantly reduced in
622 this connection, despite the commonly known medial
623 temporal lobe atrophy and the pivotal role of the hip-
624 pocampus in episodic memory encoding [36, 71].
625 However, functional and anatomical changes do not
626 necessarily overlap, and for instance, stable FC of the
627 left hippocampus in early AD (except with right lat-
628 eral prefrontal cortex) has been reported previously
629 [29].

630 Lower FC in SD than in AD (and HC) was
631 also found between the right lingual/intracalcarine
632 cortex and the left posterior hippocampus/thalamus
633 (connection no. 5). Therefore, connections between
634 bilateral lingual gyri and the left hippocampus were
635 detected in our HC sample (for illustration, see Fig. 3,
636 connections no. 4 and 5), whereas either of them were
637 damaged in SD, but not in AD. This supports the
638 recent indication of a hippocampal contribution to
639 the semantic memory network [36]. Because episodic
640 memory is relatively spared in SD, the connections
641 between the left posterior hippocampus and the bilat-
642 eral lingual gyri might contribute to the semantic
643 memory network. On the other hand, we did not find
644 an expected decrease of FC in connection no. 4 in AD,
645 although the precuneus and hippocampus contribute
646 to episodic memory, which is typically impaired in
647 AD. However, we have to bear in mind that our analy-
648 sis was restricted to temporal lobe FC and thus did not
649 cover the entire episodic memory network, including
650 brain regions located in frontal and parietal lobes. In
651 addition, no episodic memory data were available for
652 the entire sample of our study. Future studies should
653 investigate additional ROIs from the aforementioned
654 areas using larger sample sizes to tackle the increased
655 number of connections and multiple testing correc-
656 tions that are associated with larger networks.

657 The only FC reduction common to both SD and
658 AD compared with HC was found in connection
659 no. 6. The functional role of the involved regions
660 suggests an association with a frequently observed
661 clinical presentation of AD and SD characterized
662 by apathy and agitation, associated with the right
663 orbitofrontal cortex [72, 73], and impairments in
664 social behavior related to the right anterior tem-
665 poral lobe [74]. According to Olson et al. [75],
666 social knowledge is part of semantic memory and
667 involves memory about people including biographi-
668 cal information. Nonetheless, caution is advised with
669 comparing social or semantic deficits between AD
670 and SD; both symptoms have different onsets or
671 severities within disease stages, as well as different
672 characteristics. Furthermore, we did not have data on
673 social behavior or apathy/agitation of our patients.
674 Regardless, we added a common pathway to the
675 crossroad described by La Joie et al. [36]. They sug-
676 gested that the hippocampus is a converging hub of an
677 (AD-affected) episodic and a (SD-affected) semantic
678 network. Accordingly, our data indicated that besides
679 a shared damaged hub in AD and SD, the functional
680 connection between the right anterior middle/ supe-
681 rior temporal gyri and the right orbitofrontal cortex
682 might be a second candidate for the neuropathology
683 shared in both clinical populations.

684 The final significant connection (no. 7) of the
685 present study was found between the left orbitofrontal
686 cortex and the left anterior inferior and middle tem-
687 poral gyri. The literature suggests a functional role of
688 this connection in deficient socio emotional abilities
689 that are found predominantly in the behavioral variant
690 of FTD [76], and in higher level object representation,
691 involving language and auditory processing. Unlike
692 in connection no. 6, the AD group did not show an
693 impaired FC of the orbitofrontal regions with the ipsi-
694 lateral temporal cortex. Thus, one might speculate
695 about a bilateral breakdown of orbitofrontal to tem-
696 poral connections in SD, which might be related to
697 the severity of the semantic deficit.

698 This study entailed a number of study design lim-
699 itations that need to be taken into account while
700 interpreting the results. Even though the overall
701 sample size is large, the sample sizes of the three
702 subgroups are considered small (16–23 individuals).
703 Larger studies need to be conducted, however, this
704 is especially challenging for SD given its low preva-
705 lence. Therefore, we pooled two SD samples from
706 two different sites with different scanners. However,
707 most individuals of the SD group and none of the
708 AD and HC groups were from the Shanghai site,

709 which is a violation of acknowledged study design
710 standards and a potential confound. Moreover, the
711 diagnostic criteria of the two sites for SD were not
712 identical. The data from different MRI sites may have
713 different noise levels such as thermal noise, physio-
714 logical noise, and motion [52, 77]. These artifacts are
715 often global in nature, and global signal regression
716 (GSR) can successfully remove these and standard-
717 ize the data between sites and across individuals. GSR
718 can introduce negative correlations; however, GSR
719 can also improve the specificity of positive corre-
720 lations [78]. Importantly, in this study, we do not
721 interpret absolute negative correlations and solely
722 compare relative differences in correlations between
723 groups. We conducted a sensitivity analysis with the
724 study site as covariate which yielded the same results.
725 However, assumptions of independence between the
726 covariates and the patient groups were not met. The
727 present limitation of the unbalanced study design can-
728 not entirely be removed by an analysis of covariance.
729 Thus, future studies should measure different patient
730 populations across different scanner sites and ideally
731 achieve balanced groups across sites. Harmoniza-
732 tion techniques [79] can further improve data quality.
733 However, the application of harmonization methods
734 in unbalanced groups is questionable as these not
735 only eliminate scanner effects, but also the effects of
736 interest [80]. Moreover, interpretation of group differ-
737 ences between AD and SD should take into account
738 that the two dementia groups were not matched for
739 disease stage (i.e., SD showed more severe deficits
740 than AD). The sensitivity analysis with GM density
741 as covariate was in line with our results. Likewise,
742 more symptom specific behavioral scores (other than
743 MMSE) could have aided an in-depth interpretation
744 of altered FC edges in the patient groups. Lastly, our
745 analysis did not cover all brain regions potentially re-
746 levant for AD and SD. However, the choice to limit the
747 scope to the temporal lobe has three reasons: first, the
748 distinct temporal lobe atrophy is crucial for AD and
749 SD differentiation. Second, the temporal lobe is piv-
750 otal in both semantic and episodic memory functions.
751 Third, the definition of ROIs within the temporal lobe,
752 even though using an arbitrary selection threshold of
753 5% (or more) of overlap of the ROIs with any tem-
754 poral structure, may be altogether less arbitrary and
755 biased compared to subjectively selecting ROIs based
756 on expectations and literature.

757 To summarize the main findings of our study,
758 the cohort of patients with SD yielded a number of
759 distinct ipsilateral and contra lateral connections of
760 the temporal lobe that showed a significant reduc-

761 tion in FC. These connections included the regions
762 on which our predictions were based on (i.e., hip-
763 pocampus, fusiform gyrus, and temporal pole). Two
764 functional connections were intriguing due to their
765 distinctiveness from the other groups: the first was
766 the connectivity breakdown between left posterior
767 hippocampus and bilateral lingual gyri, likely reflect-
768 ing the neuronal underpinning of semantic memory
769 loss. Second, a bilateral disruption of connectivity
770 between temporal and frontal lobes was found. This
771 aligns well with the pathophysiology within the FTD
772 spectrum and especially with SD.

773 FC in AD was relatively intact compared to SD,
774 which contradicted our hypothesis. The only con-
775 nection with significantly reduced FC encompassed
776 the right orbitofrontal cortex and the right anterior
777 temporal lobe (no. 6), which we identified as an
778 AD/SD-common pathway. Additionally, Fig. 2 illus-
779 trates that our AD group had a lower FC than the HC
780 in connections no. 1, 2, and to a smaller extent no. 5
781 which all missed significance. These FC signatures in
782 the AD group could be attributed to their mild stage
783 of symptom progression (MMSE of 24.5), and poten-
784 tially an early marker of the disease, but larger and
785 longitudinal studies are needed.

786 Following the “cortically distributed plus seman-
787 tic hub” theory, several connections were found to
788 be significantly altered in the present study, which
789 affected the anterior temporal lobe – semantic hub –
790 regions (no. 1, 3, 6, and 7). Moreover, their counter-
791 parts were partly localized in the modality-specific
792 regions described by Patterson et al. [5], but also in
793 orbitofrontal regions. This agreement of our results
794 with the arguments in Patterson et al. [5] supported
795 the “distributed plus hub” theory, because we found
796 altered FC in connections between the hub and the
797 modality-specific regions. Taken together, this study
798 presents an alternative concept to investigate the
799 understanding of distinct pathophysiological changes
800 in AD and SD that are related to disruptions of func-
801 tional networks in the temporal lobe. The unique
802 aspect of our study was the definition of ROIs based
803 on functional brain segregation rather than anatomy
804 for FC analysis. Due to the comparably strict sta-
805 tistical approach and the predefined choice of ROIs,
806 our study provided a fine-grained overview of FC
807 aberration related to temporal lobe function in AD
808 and SD. However, comparability was limited owing
809 to different study sites using partially different diag-
810 nostic criteria and data acquisition procedures. We
811 emphasize here that this was an exploratory study
812 with the motivation of gathering MRI data of a rare

condition (SD) from two study sites to increase statistical power. The downside of this approach was that the retrospective characteristic caused unbalanced recording of the study groups across the two MRI scanning sites. This required the conduction of several control analyses to mitigate the occurrence of false contrasts between the groups. Thus, our findings ideally motivate future studies for replication with harmonized MRI acquisition parameters and balanced subject numbers between study sites, concurring with an optimal research practice.

DATA AVAILABILITY

Raw imaging data can be requested from the corresponding author. Aggregated data and analysis scripts to generate all results and figures are available at OSF (<https://osf.io/t4jnv/>).

ACKNOWLEDGMENTS

This work was supported by the Swedish Alzheimer fonden, the Swiss Synapsis Foundation, and the University of Bern, the Beijing Natural Science Foundation (7182088), and the NSFC (31872785). Simon Schwab acknowledges funding from the Swiss National Science Foundation (SNSF, No. 162066 and 171598).

Authors' disclosures available online (<https://www.j-alz.com/manuscript-disclosures/19-1113r2>).

SUPPLEMENTARY MATERIAL

The supplementary material is available in the electronic version of this article: <https://dx.doi.org/10.3233/JAD-191113>.

REFERENCES

- [1] Tulving E (1983) *Elements of Episodic Memory*, Oxford University Press, Oxford.
- [2] Guo CC, Gorno-Tempini ML, Gesierich B, Henry M, Trujillo A, Shany-Ur T, Jovicich J, Robinson SD, Kramer JH, Rankin KP, Miller BL, Seeley WW (2013) Anterior temporal lobe degeneration produces widespread network-driven dysfunction. *Brain* **136**, 2979–2991.
- [3] Mummery CJ, Patterson K, Price CJ, Ashburner J, Frackowiak RS, Hodges JR (2000) A voxel-based morphometry study of semantic dementia: Relationship between temporal lobe atrophy and semantic memory. *Ann Neurol* **47**, 36–45.
- [4] McClelland JL, Rogers TT (2003) The parallel distributed processing approach to semantic cognition. *Nat Rev Neurosci* **4**, 310–322.
- [5] Patterson K, Nestor PJ, Rogers TT (2007) Where do you know what you know? The representation of semantic knowledge in the human brain. *Nat Rev Neurosci* **8**, 976–987.
- [6] Hodges JR, Patterson K (2007) Semantic dementia: A unique clinicopathological syndrome. *Lancet Neurol* **6**, 1004–1014.
- [7] Landin-Romero R, Tan R, Hodges JR, Kumfor F (2016) An update on semantic dementia: Genetics, imaging, and pathology. *Alzheimers Res Ther* **8**, 52.
- [8] Collins JA, Montal V, Hochberg D, Quimby M, Mandelli ML, Makris N, Seeley WW, Gorno-Tempini ML, Dickerson BC (2017) Focal temporal pole atrophy and network degeneration in semantic variant primary progressive aphasia. *Brain* **140**, 457–471.
- [9] Bozeat S, Lambon Ralph MA, Patterson K, Garrard P, Hodges JR (2000) Non-verbal semantic impairment in semantic dementia. *Neuropsychologia* **38**, 1207–1215.
- [10] Irish M, Bunk S, Tu S, Kamminga J, Hodges JR, Hornberger M, Piguet O (2016) Preservation of episodic memory in semantic dementia: The importance of regions beyond the medial temporal lobes. *Neuropsychologia* **81**, 50–60.
- [11] Blackwell AD, Sahakian BJ, Vesey R, Semple JM, Robbins TW, Hodges JR (2004) Detecting dementia: Novel neuropsychological markers of preclinical Alzheimer's disease. *Dement Geriatr Cogn Disord* **17**, 42–48.
- [12] Mascali D, Dinuzzo M, Serra L, Mangia S, Maraviglia B, Bozzali M, Giove F (2018) Disruption of semantic network in mild Alzheimer's disease revealed by resting-state fMRI. *Neuroscience* **371**, 38–48.
- [13] Vogel A, Gade A, Stokholm J, Waldemar G (2005) Semantic memory impairment in the earliest phases of Alzheimer's disease. *Dement Geriatr Cogn Disord* **19**, 75–81.
- [14] Seeley WW, Crawford RK, Zhou J, Miller BL, Greicius MD (2009) Neurodegenerative diseases target large-scale human brain networks. *Neuron* **62**, 42–52.
- [15] Villain N, Fouquet M, Baron J-C, Mézenge F, Landeau B, de La Sayette V, Viader F, Eustache F, Desgranges B, Chételat G (2010) Sequential relationships between grey matter and white matter atrophy and brain metabolic abnormalities in early Alzheimer's disease. *Brain* **133**, 3301–3314.
- [16] Wang J, Zuo X, Dai Z, Xia M, Zhao Z, Zhao X, Jia J, Han Y, He Y (2013) Disrupted functional brain connectome in individuals at risk for Alzheimer's disease. *Biol Psychiatry* **73**, 472–481.
- [17] Liu J, Zhang X, Yu C, Duan Y, Zhuo J, Cui Y, Liu B, Li K, Jiang T, Liu Y (2016) Impaired parahippocampus connectivity in mild cognitive impairment and Alzheimer's disease. *J Alzheimers Dis* **49**, 1051–1064.
- [18] Reijmer YD, Leemans A, Caeyenberghs K, Heringa SM, Koek HL, Biessels GJ, Utrecht Vascular Cognitive Impairment Study Group (2013) Disruption of cerebral networks and cognitive impairment in Alzheimer disease. *Neurology* **80**, 1370–1377.
- [19] Tijms BM, Yeung HM, Sikkens SAM, Möller C, Smits LL, Stam CJ, Scheltens P, van der Flier WM, Barkhof F (2014) Single-subject gray matter graph properties and their relationship with cognitive impairment in early and late-onset Alzheimer's disease. *Brain Connect* **4**, 337–346.
- [20] Buckner RL, Snyder AZ, Shannon BJ, LaRossa G, Sachs R, Fotenos AF, Sheline YI, Klunk WE, Mathis CA, Morris JC, Mintun MA (2005) Molecular, structural, and functional characterization of Alzheimer's disease: Evidence for a relationship between default activity, amyloid, and memory. *J Neurosci* **25**, 7709–7717.
- [21] Poulin SP, Dautoff R, Morris JC, Barrett LF, Dickerson BC, Alzheimer's Disease Neuroimaging Initiative (2011)

- 924 Amygdala atrophy is prominent in early Alzheimer's disease and relates to symptom severity. *Psychiatry Res* **194**,
925 7–13.
- 926 [22] Burianova H, McIntosh AR, Grady CL (2010) A common
927 functional brain network for autobiographical, episodic, and
928 semantic memory retrieval. *Neuroimage* **49**, 865–874.
- 929 [23] Biswal B, Yetkin FZ, Haughton VM, Hyde JS (1995)
930 Functional connectivity in the motor cortex of resting
931 human brain using echo-planar MRI. *MagnReson Med* **34**,
932 537–541.
- 933 [24] Raichle ME, MacLeod AM, Snyder AZ, Powers WJ, Gus-
934 nard DA, Shulman GL (2001) A default mode of brain
935 function. *Proc Natl Acad Sci USA* **98**, 676–682.
- 936 [25] Broyd SJ, Demanuele C, Debener S, Helps SK, James CJ,
937 Sonuga-Barke EJS (2009) Default-mode brain dysfunction
938 in mental disorders: A systematic review. *NeurosciBiobehav*
939 *Rev* **33**, 279–296.
- 940 [26] Zhang D, Raichle ME (2010) Disease and the brain's dark
941 energy. *Nat Rev Neurol* **6**, 15–28.
- 942 [27] Greicius MD, Srivastava G, Reiss AL, Menon V (2004)
943 Default-mode network activity distinguishes Alzheimer's
944 disease from healthy aging: Evidence from functional MRI.
945 *Proc Natl Acad Sci USA* **101**, 4637–4642.
- 946 [28] Allen G, Barnard H, McColl R, Hester AL, Fields JA,
947 Weiner MF, Ringe WK, Lipton AM, Brooker M, McDon-
948 ald E, Rubin CD, Cullum CM (2007) Reduced hippocampal
949 functional connectivity in Alzheimer disease. *Arch Neurol*
950 **64**, 1482–1487.
- 951 [29] Wang L, Zang Y, He Y, Liang M, Zhang X, Tian L, Wu T,
952 Jiang T, Li K (2006) Changes in hippocampal connectivity
953 in the early stages of Alzheimer's disease: Evidence from
954 resting state fMRI. *Neuroimage* **31**, 496–504.
- 955 [30] Tahmasian M, Pasquini L, Scherr M, Meng C, Förster S,
956 MulejBratec S, Shi K, Yakushev I, Schwaiger M, Grim-
957 mer T, Diehl-Schmid J, Riedl V, Sorg C, Drzezga A (2015)
958 The lower hippocampus global connectivity, the higher
959 its local metabolism in Alzheimer disease. *Neurology* **84**,
960 1956–1963.
- 961 [31] Kobeleva X, Firbank M, Peraza L, Gallagher P, Thomas
962 A, Burn DJ, O'Brien J, Taylor JP (2017) Divergent
963 functional connectivity during attentional processing in
964 Lewy body dementia and Alzheimer's disease. *Cortex* **92**,
965 8–18.
- 966 [32] Brier MR, Thomas JB, Snyder AZ, Benzinger TL, Zhang D,
967 Raichle ME, Holtzman DM, Morris JC, Ances BM (2012)
968 Loss of intranetwork and internetwork resting state func-
969 tional connections with Alzheimer's disease progression. *J*
970 *Neurosci* **32**, 8890–8899.
- 971 [33] Ding J, Chen K, Chen Y, Fang Y, Yang Q, Lv Y, Lin N,
972 Bi Y, Guo Q, Han Z (2016) The left fusiform gyrus is a
973 critical region contributing to the core behavioral profile of
974 semantic dementia. *Front Hum Neurosci* **10**, 215.
- 975 [34] Farb NAS, Grady CL, Strother S, Tang-Wai DF, Maselis
976 M, Black S, Freedman M, Pollock BG, Campbell KL,
977 Hasher L, Chow TW (2013) Abnormal network connec-
978 tivity in frontotemporal dementia: Evidence for prefrontal
979 isolation. *Cortex* **49**, 1856–1873.
- 980 [35] Agosta F, Galantucci S, Valsasina P, Canu E, Meani A, Mar-
981 cone A, Magnani G, Falini A, Comi G, Filippi M (2014)
982 Disrupted brain connectome in semantic variant of primary
983 progressive aphasia. *Neurobiol Aging* **35**, 2646–2655.
- 984 [36] La Joie R, Landeau B, Perrotin A, Bejanin A, Egret
985 S, Pélerin A, Mézence F, Belliard S, de La Sayette V,
986 Eustache F, Desgranges B, Chételat G (2014) Intrinsic
987 connectivity identifies the hippocampus as a main crossroad
988 between Alzheimer's and semantic dementia-targeted net-
989 works. *Neuron* **81**, 1417–1428.
- 990 [37] Margulies DS, Kelly AMC, Uddin LQ, Biswal BB, Castellan-
991 os FX, Milham MP (2007) Mapping the functional
992 connectivity of anterior cingulate cortex. *Neuroimage* **37**,
993 579–588.
- 994 [38] Craddock RC, James GA, Holtzheimer PE 3rd, Hu XP, May-
995 berg HS (2012) A whole brain fMRI atlas generated via
996 spatially constrained spectral clustering. *Hum Brain Mapp*
997 **33**, 1914–1928.
- 998 [39] Henke K (2010) A model for memory systems based on pro-
999 cessing modes rather than consciousness. *Nat Rev Neurosci*
1000 **11**, 523–532.
- 1001 [40] Duss SB, Reber TP, Hänggi J, Schwab S, Wiest R, Müri
1002 RM, Brugger P, Gutbrod K, Henke K (2014) Unconscious
1003 relational encoding depends on hippocampus. *Brain* **137**,
1004 3355–3370.
- 1005 [41] Orban P, Dansereau C, Desbois L, Mongeau-Pérusse V,
1006 Giguère C-É, Nguyen H, Mendrek A, Stip E, Bellec P (2018)
1007 Multisite generalizability of schizophrenia diagnosis clas-
1008 sification based on functional brain connectivity. *Schizophr*
1009 *Res* **192**, 167–171.
- 1010 [42] Neary D, Snowden JS, Gustafson L, Passant U, Stuss D,
1011 Blythe S, Freedman M, Kertesz A, Robert PH, Albert M,
1012 Boone K, Miller BL, Cummings J, Benson DF (1998)
1013 Frontotemporal lobar degeneration: A consensus on clinical
1014 diagnostic criteria. *Neurology* **51**, 1546–1554.
- 1015 [43] Gorno-Tempini ML, Hillis AE, Weintraub S, Kertesz A,
1016 Mendez M, Cappa SF, Ogar JM, Rohrer JD, Black S, Boeve
1017 BF, Manes F, Dronkers NF, Vandenberghe R, Rascovsky K,
1018 Patterson K, Miller BL, Knopman DS, Hodges JR, Mesulam
1019 MM, Grossman M (2011) Classification of primary progres-
1020 sive aphasia and its variants. *Neurology* **76**, 1006–1014.
- 1021 [44] World Health Organization (2004) *International Statistical*
1022 *Classification of Diseases and Related Health Problems*,
1023 World Health Organization.
- 1024 [45] Grieder M, Crinelli RM, Jann K, Federspiel A, Wirth M,
1025 Koenig T, Stein M, Wahlund LO, Dierks T (2013) Correla-
1026 tion between topographic N400 anomalies and reduced
1027 cerebral blood flow in the anterior temporal lobes of patients
1028 with dementia. *J Alzheimers Dis* **36**, 711–731.
- 1029 [46] Andreotti J, Dierks T, Wahlund LO, Grieder M (2017)
1030 Diverging progression of network disruption and atrophy in
1031 Alzheimer's disease and semantic dementia. *J Alzheimers*
1032 *Dis* **55**, 981–993.
- 1033 [47] Chen Y, Chen K, Ding J, Zhang Y, Yang Q, Lv Y, Guo Q,
1034 Han Z (2017) Brain network for the core deficits of semantic
1035 dementia: A neural network connectivity-behavior mapping
1036 study. *Front Hum Neurosci* **11**, 267.
- 1037 [48] Afyouni S, Nichols TE (2018) Insight and inference for
1038 DVARS. *Neuroimage* **172**, 291–312.
- 1039 [49] Power JD, Barnes KA, Snyder AZ, Schlaggar BL, Petersen
1040 SE (2012) Spurious but systematic correlations in func-
1041 tional connectivity MRI networks arise from subject motion.
1042 *Neuroimage* **59**, 2142–2154.
- 1043 [50] Hurley RS, Bonakdarpour B, Wang X, Mesulam M-M
1044 (2015) Asymmetric connectivity between the anterior tem-
1045 poral lobe and the language network. *J CognNeurosci* **27**,
1046 464–473.
- 1047 [51] Maldjian JA, Laurienti PJ, Kraft RA, Burdette JH (2003) An
1048 automated method for neuroanatomic and cytoarchitectonic
1049 atlas-based interrogation of fMRI data sets. *Neuroimage* **19**,
1050 1233–1239.
- 1051 [52] Power JD, Mitra A, Laumann TO, Snyder AZ, Schlaggar
1052 BL, Petersen SE (2014) Methods to detect, characterize, and
1053

- remove motion artifact in resting state fMRI. *Neuroimage* **84**, 320–341.
- [53] Chang C, Glover GH (2009) Effects of model-based physiological noise correction on default mode network anti-correlations and correlations. *Neuroimage* **47**, 1448–1459.
- [54] Murphy K, Birn RM, Bandettini PA (2013) Resting-state fMRI confounds and cleanup. *Neuroimage* **80**, 349–359.
- [55] Miller GA, Chapman JP (2001) Misunderstanding analysis of covariance. *J AbnormPsychol* **110**, 40–48.
- [56] Ashburner J, Friston KJ (2000) Voxel-based morphometry—the methods. *Neuroimage* **11**, 805–821.
- [57] Gaser C, Dahnke R (2016) CAT-a computational anatomy toolbox for the analysis of structural MRI data. *Hum Brain Mapp* **2016**, 336–348.
- [58] Friston KJ, Ashburner JT, Kiebel SJ, Penny WD, Nichols TE (2007) *Statistical Parametric Mapping: The Analysis of Functional Brain Images*, Elsevier Science.
- [59] McDonough IM, Nashiro K (2014) Network complexity as a measure of information processing across resting-state networks: Evidence from the Human Connectome Project. *Front HumNeurosci* **8**, 409.
- [60] Sormaz M, Jefferies E, Bernhardt BC, Karapanagiotidis T, Mollo G, Bernasconi N, Bernasconi A, Hartley T, Smallwood J (2017) Knowing what from where: Hippocampal connectivity with temporoparietal cortex at rest is linked to individual differences in semantic and topographic memory. *Neuroimage* **152**, 400–410.
- [61] Shtyrov Y, Pulvermüller F (2007) Early MEG activation dynamics in the left temporal and inferior frontal cortex reflect semantic context integration. *J CognNeurosci* **19**, 1633–1642.
- [62] Jobard G, Crivello F, Tzourio-Mazoyer N (2003) Evaluation of the dual route theory of reading: A meta-analysis of 35 neuroimaging studies. *Neuroimage* **20**, 693–712.
- [63] Wirth M, Horn H, Koenig T, Razafimandimby A, Stein M, Mueller T, Federspiel A, Meier B, Dierks T, Strik W (2008) The early context effect reflects activity in the temporo-prefrontal semantic system: Evidence from electrical neuroimaging of abstract and concrete word reading. *Neuroimage* **42**, 423–436.
- [64] Mesulam M-M, Thompson CK, Weintraub S, Rogalski EJ (2015) The Wernicke conundrum and the anatomy of language comprehension in primary progressive aphasia. *Brain* **138**, 2423–2437.
- [65] Nilakantan AS, Voss JL, Weintraub S, Mesulam M-M, Rogalski EJ (2017) Selective verbal recognition memory impairments are associated with atrophy of the language network in non-semantic variants of primary progressive aphasia. *Neuropsychologia* **100**, 10–17.
- [66] Brunyé TT, Moran JM, Holmes A, Mahoney CR, Taylor HA (2017) Non-invasive brain stimulation targeting the right fusiform gyrus selectively increases working memory for faces. *Brain Cogn* **113**, 32–39.
- [67] Rangarajan V, Hermes D, Foster BL, Weiner KS, Jacques C, Grill-Spector K, Parvizi J (2014) Electrical stimulation of the left and right human fusiform gyrus causes different effects in conscious face perception. *J Neurosci* **34**, 12828–12836.
- [68] Mion M, Patterson K, Acosta-Cabronero J, Pengas G, Izquierdo-Garcia D, Hong YT, Fryer TD, Williams GB, Hodges JR, Nestor PJ (2010) What the left and right anterior fusiform gyri tell us about semantic memory. *Brain* **133**, 3256–3268.
- [69] Owen AM, Milner B, Petrides M, Evans AC (1996) A specific role for the right parahippocampal gyrus in the retrieval of object-location: A positron emission tomography study. *J CognNeurosci* **8**, 588–602.
- [70] Luck D, Danion J-M, Marrer C, Pham B-T, Gounot D, Foucher J (2010) The right parahippocampal gyrus contributes to the formation and maintenance of bound information in working memory. *Brain Cogn* **72**, 255–263.
- [71] Tondelli M, Wilcock GK, Nichelli P, De Jager CA, Jenkinson M, Zamboni G (2012) Structural MRI changes detectable up to ten years before clinical Alzheimer’s disease. *Neurobiol Aging* **33**, 825.e25–36.
- [72] Bruen PD, McGeown WJ, Shanks MF, Venneri A (2008) Neuroanatomical correlates of neuropsychiatric symptoms in Alzheimer’s disease. *Brain* **131**, 2455–2463.
- [73] Fernández-Matarrubia M, Matías-Guiú JA, Cabrera-Martín MN, Moreno-Ramos T, Valles-Salgado M, Carreras JL, Matías-Guiú J (2018) Different apathy clinical profile and neural correlates in behavioral variant frontotemporal dementia and Alzheimer’s disease. *Int J Geriatr Psychiatry* **33**, 141–150.
- [74] Kumfor F, Landin-Romero R, Devenney E, Hutchings R, Grasso R, Hodges JR, Piguet O (2016) On the right side? A longitudinal study of left- versus right-lateralized semantic dementia. *Brain* **139**, 986–998.
- [75] Olson IR, McCoy D, Klobusicky E, Ross LA (2013) Social cognition and the anterior temporal lobes: A review and theoretical framework. *SocCogn Affect Neurosci* **8**, 123–133.
- [76] Dermody N, Wong S, Ahmed R, Piguet O, Hodges JR, Irish M (2016) Uncovering the neural bases of cognitive and affective empathy deficits in Alzheimer’s disease and the behavioral-variant of frontotemporal dementia. *J Alzheimers Dis* **53**, 801–816.
- [77] Birn RM (2012) The role of physiological noise in resting-state functional connectivity. *Neuroimage* **62**, 864–870.
- [78] Murphy K, Fox MD (2017) Towards a consensus regarding global signal regression for resting state functional connectivity MRI. *Neuroimage* **154**, 169–173.
- [79] Yu M, Linn KA, Cook PA, Phillips ML, McInnis M, Fava M, Trivedi MH, Weissman MM, Shinohara RT, Sheline YI (2018) Statistical harmonization corrects site effects in functional connectivity measurements from multi-site fMRI data. *Hum Brain Mapp* **39**, 4213–4227.
- [80] Yamashita A, Yahata N, Itahashi T, Lisi G, Yamada T, Ichikawa N, Takamura M, Yoshihara Y, Kunimatsu A, Okada N, Yamagata H, Matsuo K, Hashimoto R, Okada G, Sakai Y, Morimoto J, Narumoto J, Shimada Y, Kasai K, Kato N, Takahashi H, Okamoto Y, Tanaka SC, Kawato M, Yamashita O, Imamizu H (2019) Harmonization of resting-state functional MRI data across multiple imaging sites via the separation of site differences into sampling bias and measurement bias. *PLoSBIol* **17**, e3000042.
- [81] Welch LW, Doineau D, Johnson S, King D (1996) Educational and gender normative data for the Boston naming test in a group of older adults. *Brain Lang* **53**, 260–266.
- [82] Tombaugh TN, Kozak J, Rees L (1999) Normative data stratified by age and education for two measures of verbal fluency: FAS and animal naming. *Arch ClinNeuropsychol* **14**, 167–177.
- [83] Woods SP, Scott JC, Sires DA, Grant I, Heaton RK, Tröster AI, HIV Neurobehavioral Research Center Group (2005) Action (verb) fluency: Test-retest reliability, normative standards, and construct validity. *J IntNeuropsycholSoc* **11**, 408–415.